JOURNAL OF GUIDANCE, CONTROL, AND DYNAMICS
Vol. 30, No. 6, November–December 2007

Elastic Oscillations of the Space Elevator Ribbon

Stephen S. Cohen* and Arun K. Misra†
McGill University, Montreal, Quebec H3A 2K6, Canada

DOI: 10.2514/1.29010

The space elevator is likely to offer an alternate and efficient method for space travel. The main component of the space elevator is the tether (or the ribbon), which extends from the Earth to an equatorial satellite beyond the geosynchronous altitude and is fixed to a base on the surface of the Earth at its lower end. This paper studies the elastic oscillations of this ribbon. The elastic deformations are discretized using a set of admissible basis functions, and the Lagrangian approach is used to derive the equations of motion of this discrete system. For small motions, the longitudinal extension and transverse displacement of the ribbon can be analyzed separately. Longitudinal and transverse modal frequencies and corresponding modes are calculated numerically, assuming typical values for the properties of the ribbon.

Nomenclature

A	=	cross-sectional area of the ribbon
$A_i(t)$	=	nondimensional generalized coordinates associated with longitudinal extension
A_m	=	maximum cross-sectional area of the ribbon
A_0	=	cross-sectional area of the ribbon at the base
$a_i(t)$	=	generalized coordinates associated with longitudinal extension
$B_i(t)$	=	nondimensional generalized coordinates associated with transverse motion
$b_i(t)$	=	generalized coordinates associated with transverse motion
E	=	modulus of elasticity of the ribbon material
g_0	=	surface gravity of the Earth
$\bar{h}$	=	characteristic height of the ribbon
L	=	nominally stretched length of the ribbon
L_0	=	nominal length of the ribbon
M	=	number of assumed modes for transverse motion
M_c	=	nondimensional mass of the counterweight (ballast)
M_p	=	nondimensional measure of mass of the tether (ribbon)
m_c	=	mass of the counterweight (ballast)
m_t	=	mass of the tether (ribbon)
m_{tot}	=	total mass of the system
N	=	number of assumed modes for longitudinal extension
R_E	=	radius of the Earth
R_G	=	synchronous orbit radius of the Earth
s	=	position on the ribbon
t	=	time
U	=	nondimensional longitudinal extension of the tether along the reference line
u	=	longitudinal extension of the tether along the reference line
V	=	nondimensional transverse motion of the tether relative to the reference line
v	=	transverse motion of the tether relative to the reference line
α	=	angle between the local vertical and reference lines (libration angle)
β	=	ratio of the geosynchronous radius to the radius of the Earth
γ	=	bulk density of the ribbon material
ε_0	=	nominal strain in the ribbon
Λ	=	ratio of nominal ribbon length to the radius of the Earth
μ	=	gravitational constant of the Earth
ξ	=	nondimensional position on the ribbon
σ_0	=	nominal stress in the ribbon
τ	=	nondimensional time
ϕ_i	=	basis functions associated with transverse motion
ψ_i	=	basis functions associated with longitudinal extension
Ω	=	spin rate of the Earth
$\bar{\Omega}$	=	characteristic frequency ratio

I. Introduction

AS the number of satellite launches increases, the implementation of a more efficient method of space travel becomes very desirable. An alternate method used to escape the gravitational pull of the Earth may be the space elevator. The concept of the space elevator originated in the late 19th century: Tsiolkovsky [1] was the first to document it. The first modern ideas of the space elevator came from Artsutanov [2] and Isaacs et al. [3]. However, not much attention was paid to the subject until Pearson [4] published his paper about the orbital tower. He showed that a great deal of tension would manifest within the ribbon due to the large gravitational and centripetal forces acting on it in opposite directions. He also derived the taper function for the ribbon that would provide constant stress throughout it. It was made clear in Pearson's paper that for the space elevator to ever become a reality, the use of a material having a much higher strength-to-density ratio than that of steel would be necessary. Although Pearson laid the foundation for the properties of a space elevator, there was little continuation of this research for many years, until Iijima [5] discovered a new material composed of hexagonal arrays of carbon atoms; the material is known as carbon nanotube. The discovery of carbon nanotubes, which might be a suitable material for the space elevator ribbon, has increased the likelihood that a space elevator will be constructed in the foreseeable future. With the progression of this technology, studying other aspects of the space elevator, such as its dynamics, becomes appropriate [6].

Only a few dynamic studies of the space elevator exist. McInnes [7] obtained analytical results for the simplest case of a space elevator: a point-mass climber traversing a stationary ribbon. Lang [8] used tether-simulation software to obtain numerical results for the motion and internal stress of the ribbon in response to ascending climbers and aerodynamic loads. Finally, Patamia and Jorgensen [9] developed an analytical model for studying the transverse displacement of the tether. With some approximation, they obtained the mode shapes associated with its transverse displacement; these mode shapes were sinusoidal in nature. In this paper, the problem is handled in a more complete and accurate manner: both longitudinal

Received 24 November 2006; revision received 11 April 2007; accepted for publication 17 April 2007.

*Research Assistant, Department of Mechanical Engineering.
†Thomas Workman Professor, Department of Mechanical Engineering. Associate Fellow AIAA.

and transverse oscillations are considered. The elastic displacements are discretized using a set of admissible basis functions and Lagrange's equations are used to derive the equations of motion.

II. Description of the System

The space elevator model consists of a ribbon and counterweight and is depicted in Fig. 1; the model is in the equatorial plane. The center of the Earth is assumed to be inertially fixed; the origin of the inertial frame coincides with this point. The angular velocity of the system Ω is equal to the rotation rate of the Earth. Its period is approximated to be 24 h (although, strictly speaking, the sidereal period is slightly less than that). The rotating unit vectors $\mathbf{e_v}$ and $\mathbf{e_h}$ point in the local vertical and horizontal directions, respectively. Unit vector $\mathbf{i}$ is along the reference line, which extends from the base to the counterweight. The unit vectors $\mathbf{i}$ and $\mathbf{j}$ are obtained by rotating $\mathbf{e_v}$ and $\mathbf{e_h}$ through an angle α. This rotation of the reference line is defined as the libration angle. The distance of a ribbon element before deformation from the base of the elevator is denoted by s. The base of the elevator is attached to the surface of the Earth in this study. Longitudinal and transverse displacements of this element are denoted by u and v, respectively. The ribbon has nominal (unstressed) length L_0. There will be a counterweight at the space end of the ribbon, for which the mass is denoted here by m_c. The ribbon's cross-sectional area profile, which varies along the length of the ribbon, will be derived next.

III. Static Deformation of the Ribbon

Before elastic oscillations can be considered, it is necessary to examine the static deformation of the ribbon. The nominally deformed configuration of the space elevator is defined by $\alpha = v(s) = 0$ and $u(s) = u_0(s)$. Pearson [4] showed that an ideal ribbon design would have constant stress across its length, and he derived an appropriate area of cross-sectional tapering function. However, he did not take the longitudinal extension caused by the tension in the static ribbon into account when deriving this function. A more accurate expression for the cross-sectional area profile is now sought. The tension in the static ribbon will cause it to extend longitudinally from its unstressed state by $u_0(s)$. The nominal strain in the ribbon is given by

$$\varepsilon_0 = \mathrm{d}u_0/\mathrm{d}s = \sigma_0/E \tag{1}$$

where σ_0 is the nominal stress in the ribbon and E is the modulus of elasticity of the ribbon material. Using zero deformation at the base as a boundary condition, the deformation of the static ribbon from its nominal unstressed state is given by $u_0(s) = \varepsilon_0 s$. Thus, if the nominally stretched ribbon is to have length L, its original length must be given by $L_0 = L/(1 + \varepsilon_0)$. It is noted that even for a small nominal strain, the difference between the ribbon length before and after deployment would be thousands of kilometers, because the nominal strain will be of the order of 10^{-2} and the length of the ribbon will be of the order of 10^5 km.

Consider an element $\mathrm{d}m$ at a distance r from the center of the Earth. The forces acting on the element are shown in Fig. 2. T is the tension

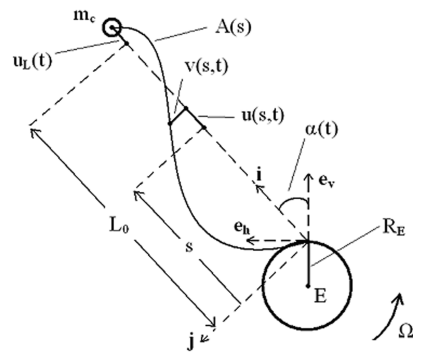

Fig. 1 A schematic diagram of the space elevator.

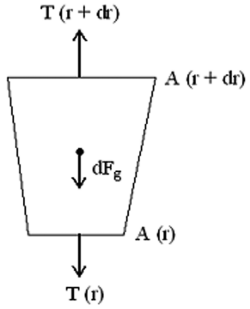

Fig. 2 Free-body diagram of a ribbon element.

in the ribbon and $\mathrm{d}F_g$ is the gravitational force acting on the element. From Newton's second law,

$$\mathrm{d}ma_r = \sum F_r = T(r + \mathrm{d}r) - T(r) - \mathrm{d}F_g \tag{2}$$

Substituting values for tension, gravitational force, and acceleration,

$$\mathrm{d}m(-\Omega^2 r) = \sigma_0 A(r + \mathrm{d}r) - \sigma_0 A(r) - \mathrm{d}m(\mu/r^2) \tag{3}$$

where $\mathrm{d}m$ is the product of the bulk density, and the infinitesimal volume given by $A\,\mathrm{d}s$ and μ is the gravitational constant of the Earth. The spatial coordinate r and the ribbon coordinate s are related by

$$r = R_E + s + u_0(s) = R_E + s(1 + \varepsilon_0) \tag{4}$$

where R_E is the radius of the Earth. Making the preceding substitutions and then simplifying, Eq. (3) becomes

$$\gamma A(s)\,\mathrm{d}s\{\mu/[R_E + s(1 + \varepsilon_0)]^2 - \Omega^2[R_E + s(1 + \varepsilon_0)]\} = \sigma_0\,\mathrm{d}A \tag{5}$$

It is now useful to introduce the characteristic height of the ribbon, which is defined by $\bar{h} = \sigma_0/\gamma g_0$. Here, g_0 is the surface gravity of the Earth and is equal to μ/R_E^2. The characteristic height is a measure of the strength-to-density ratio of the ribbon material, scaled with respect to the surface gravity of the Earth to have a unit of length.

Substituting $\Omega^2 = \mu/R_G^3$ (where R_G is the geosynchronous orbit radius), $\mu = g_0 R_E^2$, and $\sigma_0 = \bar{h}\gamma g_0$ into Eq. (5) and then simplifying, one arrives at

$$\frac{\mathrm{d}A}{A} = \frac{R_E^2}{\bar{h}}\left\{\frac{1}{[R_E + s(1 + \varepsilon_0)]^2} - \frac{R_E + s(1 + \varepsilon_0)}{R_G^3}\right\}\mathrm{d}s \tag{6}$$

Integrating Eq. (6) results in

$$A(s) = c\exp\left(-\frac{R_E^2}{\bar{h}(1 + \varepsilon_0)}\left\{\frac{1}{R_E + s(1 + \varepsilon_0)} + \frac{[R_E + s(1 + \varepsilon_0)]^2}{2R_G^3}\right\}\right) \tag{7}$$

where c is a constant of integration. The boundary condition for the preceding equation is that the net force acting on its free end must be equal to the tension $(\sigma_0 A(s)|_{s=L_0})$ in it at that point. Because there is no net force acting at that point, this boundary condition could only be satisfied by having the area of cross section equal to zero there (this would ensure zero tension). However, from Eq. (7), it is clear that the area of cross section of the ribbon cannot be zero at *any* location for this case of constant stress. Thus, to satisfy the boundary condition at the tip of the ribbon, a mass m_c (the counterweight) must be attached there. The forces acting on the counterweight can be made equal to the tension at the tip by forcing

$$m_c[\Omega^2(R_E + L) - \mu/(R_E + L)^2] = \sigma_0 A(s)|_{s=L_0} \tag{8}$$

Through differentiation of Eq. (7), it may be shown that the maximum value of area of cross section occurs at the location $s = (R_G - R_E)/(1 + \varepsilon_0)$, which corresponds to the radial position

$r = R_G$. The area at this location may be set to the useful design parameter A_m, which is the maximum area of cross section of the ribbon and is a free design parameter. Then after some manipulation, the cross-sectional area profile may be expressed as

$$A(s) = A_m \exp[F(s)] \tag{9}$$

where

$$F(s) = \frac{R_E^2}{\bar{h} R_G (1+\varepsilon_0)} \left(\frac{3}{2} - \frac{R_G}{R_E + s(1+\varepsilon_0)} - \frac{[R_E + s(1+\varepsilon_0)]^2}{2R_G^2} \right) \tag{10}$$

or, equivalently,

$$A(r) = A_m \exp\left[\frac{R_E^2}{\bar{h} R_G (1+\varepsilon_0)} \left(\frac{3}{2} - \frac{R_G}{r} - \frac{r^2}{2R_G^2} \right) \right] \tag{11}$$

An almost identical solution as that given in Eq. (11) was obtained by Pearson [4] . The only difference is that the $(1 + \varepsilon_0)$ term did not appear in his solution, because the nominal strain was not considered in his taper-function derivation. Because the nominal strain is not negligible, this modification to the profile of the area of cross section is essential. Also, in Pearson's derivation, the boundary condition at the tip of the ribbon was not considered. It is essential that there be a counterweight placed at the free end, and from Eq. (8) it is given by

$$m_c = \frac{\sigma_0 A_m \exp[F(s)]|_{s=L_0}}{\{\Omega^2 [R_E + L_0(1+\varepsilon_0)] - \mu / [R_E + L_0(1+\varepsilon_0)]^2\}} \tag{12}$$

The resulting taper ratio of the ribbon, which is defined here as the quotient of A_m and the area of cross section at the Earth's surface A_0, is given by

$$A_m / A_0 = \exp\left[\frac{R_E}{\bar{h}(1+\varepsilon_0)} \left(1 - \frac{R_E}{R_G}\right)^2 \left(1 + \frac{R_E}{2R_G}\right) \right] \tag{13}$$

Hence, for a material with $\bar{h} = 2762$ km and $E = 1000$ GPa, the taper ratio is exactly 6. The taper function of a material having these values is plotted in Fig. 3. From [10], the density of carbon nanotubes is 1300 kg/m^3, its Young's modulus is 1000 GPa, and the theoretical value for its maximum tensile strength is 130 GPa. However, this strength property has yet to be attained in practice. Still, if the maximum strength of the ribbon material were only 70 GPa, its characteristic height would be 2762 km using a safety factor of about two ($\sigma_0 = 35.2$ GPa), and the variation in area of cross section would be as shown in Fig. 3.

The nominal tension in the ribbon may now be expressed as

$$T_0(s) = \sigma_0 A(s) = \sigma_0 A_m \exp[F(s)] \tag{14}$$

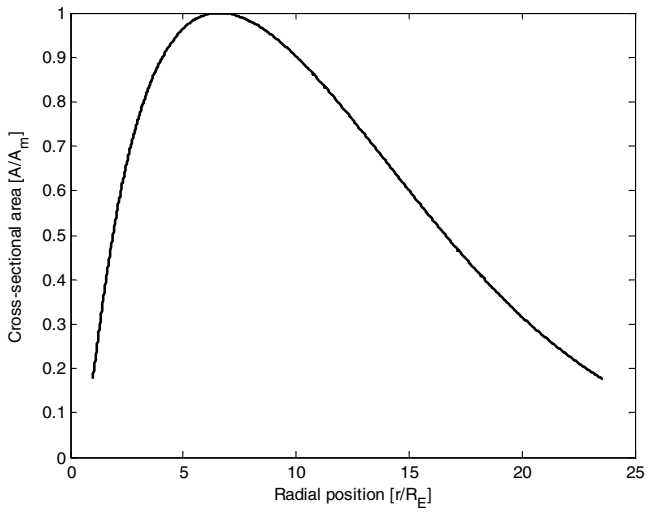

Fig. 3 Cross-sectional area profile of the ribbon for $\bar{h} = 2762$ km.

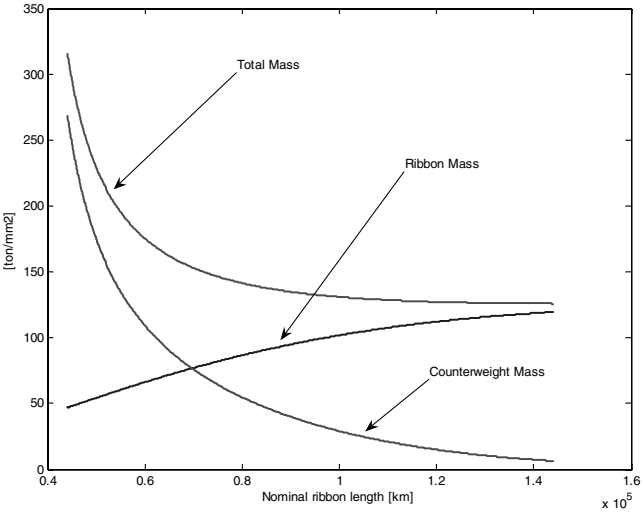

Fig. 4 Ribbon, counterweight, and total mass per unit area A_m of the ribbon vs nominal ribbon length; the taper ratio is 6.

The mass of the ribbon is given by

$$m_t = \gamma A_m \int_0^{L_0} \exp[F(s)]\, \mathrm{d}s \tag{15}$$

Through manipulation of Eq. (12), the required counterweight may be expressed as

$$m_c = \gamma A_m \bar{h} \frac{\exp[F(s)|_{s=L_0}]}{(R_E/R_G)^2 ([R_E + L_0(1+\varepsilon_0)]/R_G - \{R_G/[R_E + L_0(1+\varepsilon_0)]\}^2)} \tag{16}$$

Clearly, the required counterweight is proportional to the maximum area of cross section of the ribbon and is also dependent on other material and design parameters. In Fig. 4, the ribbon, counterweight, and total mass per maximum unit area of cross section of the ribbon is plotted against the nominal ribbon length, assuming a taper ratio of 6 (ribbon material parameters are as assumed earlier). A ribbon with $L_0 = 100,000$ km and $A_m = 10$ mm^2 would have a mass of about 1000 tons. The corresponding counterweight mass would be about 300 tons.

IV. Elastic Oscillations of the Ribbon

Both longitudinal and transverse displacements of the ribbon, u and v, are expanded in series form as products of a set of generalized coordinates and spatial basis functions. The longitudinal extension is expressed as

$$u(s,t) = \varepsilon_0 s + \sum_{i=1}^{N} a_i(t) \psi_i(s) \tag{17}$$

where N generalized coordinates $a_i(t)$ and appropriate basis functions $\psi_i(s)$ (to be chosen later) are used to describe the extension of the ribbon from its nominal amount $u_0(s) = \varepsilon_0 s$. Because an energy method will be used to derive the equations of motion, $\psi_i(s)$ need to be only admissible functions, not comparison functions [i.e., they need to satisfy only the geometric boundary condition $\psi_i(0) = 0$].

The transverse displacement is represented as

$$v(s,t) = \sum_{i=1}^{M} b_i(t) \phi_i(s) \tag{18}$$

where M generalized coordinates $b_i(t)$ are used to describe this displacement. Again, $\phi_i(s)$ are appropriate admissible basis functions to be chosen later, satisfying the geometric boundary

conditions $\phi_i(0) = \phi_i(L_0) = 0$. Generalized coordinates α, a_i $(i = 1, 2, \ldots, N)$, and b_i $(i = 1, 2, \ldots, M)$ fully define this $N + M + 1$ degree-of-freedom system.

The position vectors of a ribbon element and the counterweight with respect to the center of the Earth, respectively, are given by

$$\mathbf{r}_\mathbf{R}(s) = (R_E \cos\alpha + s + u)\mathbf{i} + (v - R_E \sin\alpha)\mathbf{j} \tag{19}$$

and

$$\mathbf{r}_\mathbf{C} = (R_E \cos\alpha + L_0 + u_L)\mathbf{i} - R_E \sin\alpha\mathbf{j} \tag{20}$$

where

$$u_L = u(L_0, t) \tag{21}$$

The velocity vectors relative to the inertial frame are given by

$$\mathbf{v}_\mathbf{R}(s) = [R_E\Omega \sin\alpha + \dot{u} - (\Omega + \dot{\alpha})v]\mathbf{i} + [R_E\Omega \cos\alpha + \dot{v} + (\Omega + \dot{\alpha})(s + u)]\mathbf{j} \tag{22}$$

and

$$\mathbf{v}_\mathbf{C} = [R_E\Omega \sin\alpha + \dot{u}_L]\mathbf{i} + [R_E\Omega \cos\alpha + (\Omega + \dot{\alpha})(L_0 + u_L)]\mathbf{j} \tag{23}$$

The total kinetic energy of the system can then be written as

$$K = \frac{1}{2}\gamma \int_0^{L_0} A(s)[\mathbf{v}_\mathbf{R}(s) \bullet \mathbf{v}_\mathbf{R}(s)]\,\mathrm{d}s + \frac{1}{2}m_c(\mathbf{v}_\mathbf{C} \bullet \mathbf{v}_\mathbf{C}) \tag{24}$$

The total potential energy of the system is given by

$$P = -\mu\gamma \int_0^{L_0} \frac{A(s)}{\sqrt{\mathbf{r}_\mathbf{R}(s) \bullet \mathbf{r}_\mathbf{R}(s)}} - \frac{\mu m_c}{\sqrt{\mathbf{r}_\mathbf{C} \bullet \mathbf{r}_\mathbf{C}}} + P_{\mathrm{st}} \tag{25}$$

where the strain energy stored in the ribbon, P_{st}, is given by

$$P_{\mathrm{st}} = \frac{1}{2}E \int_0^{L_0} A(s)\left[\left(\frac{\partial u}{\partial s}\right)^2 + \frac{\partial u}{\partial s}\left(\frac{\partial v}{\partial s}\right)^2 + \frac{1}{2}\left(\frac{\partial v}{\partial s}\right)^4 - \left(\frac{\partial u}{\partial s}\right)^2\left(\frac{\partial v}{\partial s}\right)^2\right]\mathrm{d}s \tag{26}$$

Min et al. [11] derived the strain energy expression for three-dimensional motion, neglecting fifth-order and higher terms. A linear stress–strain relation was assumed in deriving it. Equation (26) is obtained from that expression after the out-of-plane deformation is set to zero. Because the longitudinal extension includes the nominal extension caused by the nominal strain in the ribbon, the general strain energy term includes the nominal strain energy.

For a system without external excitations, Lagrange's equations can be written as

$$\frac{\mathrm{d}}{\mathrm{d}t}\left[\frac{\partial K}{\partial \dot{q}_i}\right] - \frac{\partial K}{\partial q_i} + \frac{\partial P}{\partial q_i} = 0 \tag{27}$$

In Eq. (27), q_i is a generalized coordinate. By substituting the energy expressions from Eqs. (24) and (25) into Eq. (27) and letting the generalized coordinates be the degrees of freedom of the space elevator, one obtains the $N + M + 1$ equations of motion of the system. For convenience, all of the equations of motion are nondimensionalized. Nondimensional masses are defined by

$$M_p = \gamma A_m L_0/m_{\mathrm{tot}}, \qquad M_c = m_c/m_{\mathrm{tot}} \tag{28}$$

where the total mass of the system is given by $m_{\mathrm{tot}} = m_t + m_c$. The displacements are also nondimensionalized and are defined by

$$U = u/L_0 = \varepsilon_0\xi + \sum_{i=1}^{N} A_i(\tau)\psi_i(\xi) \tag{29}$$

and

$$V = v/L_0 = \sum_{i=1}^{M} B_i(\tau)\phi_i(\xi) \tag{30}$$

where

$$A_i = a_i/L_0, \qquad B_i = b_i/L_0, \qquad \xi = s/L_0 \tag{31}$$

and nondimensional time is defined by

$$\tau = \Omega t \tag{32}$$

The nondimensionalized equations of motion for α, A_k $(k = 1, 2, \ldots, N)$, and B_k $(k = 1, 2, \ldots, M)$ are, respectively,

$$\begin{aligned}
&\left\{M_c(1 + U_1)^2 + M_p \int_0^1 \exp[F(\xi)][(\xi + U)^2 + V^2]\,\mathrm{d}\xi\right\}\alpha'' \\
&\quad + M_p \int_0^1 \exp[F(\xi)][(\xi + U)V'' - VU'']\,\mathrm{d}\xi \\
&\quad + \frac{1}{\Lambda}\left\{M_p \int_0^1 \exp[F(\xi)](\xi + U)\,\mathrm{d}\xi + M_c(1 + U_1)\right\}\sin\alpha \\
&\quad + 2(1 + \alpha')\left\{M_c(1 + U_1)U_1' + M_p \int_0^1 \exp[F(\xi)][(\xi + U)U' + VV']\,\mathrm{d}\xi\right\} + \frac{1}{\Lambda}M_p \int_0^1 \exp[F(\xi)]V\,\mathrm{d}\xi\cos\alpha \\
&\quad - \frac{\beta^3 M_p}{\Lambda}\int_0^1 \frac{\exp[F(\xi)][(\xi + U)\sin\alpha + V\cos\alpha]}{\{[\cos\alpha + \Lambda(\xi + U)]^2 + [\Lambda V - \sin\alpha]^2\}^{\frac{3}{2}}}\,\mathrm{d}\xi \\
&\quad - \frac{\beta^3 M_c}{\Lambda}\frac{(1 + U_1)\sin\alpha}{\{[\cos\alpha + \Lambda(1 + U_1)^2] + \sin^2\alpha\}^{\frac{3}{2}}} = 0
\end{aligned} \tag{33}$$

$$\begin{aligned}
&M_p \int_0^1 \exp[F(\xi)]\psi_k U''\,\mathrm{d}\xi + M_c\psi_{k1}U_1'' \\
&\quad - M_p \int_0^1 \exp[F(\xi)]\psi_k V\,\mathrm{d}\xi\alpha'' \\
&\quad - 2M_p(1 + \alpha')\int_0^1 \exp[F(\xi)]\psi_k V'\,\mathrm{d}\xi \\
&\quad - M_p(1 + \alpha')^2 \int_0^1 \exp[F(\xi)]\psi_k(\xi + U)\,\mathrm{d}\xi \\
&\quad - M_c\psi_{k1}(1 + \alpha')^2(1 + U_1) \\
&\quad - \frac{1}{\Lambda}\left\{M_p \int_0^1 \exp[F(\xi)]\psi_k\,\mathrm{d}\xi + M_c\psi_{k1}\right\}\cos\alpha \\
&\quad + \beta^3 M_p \int_0^1 \frac{\exp[F(\xi)][(1/\Lambda)\cos\alpha + \xi + U]\psi_k}{\{[\cos\alpha + \Lambda(\xi + U)]^2 + [\Lambda V - \sin\alpha]^2\}^{\frac{3}{2}}}\,\mathrm{d}\xi \\
&\quad + \beta^3 M_c \frac{[(1/\Lambda)\cos\alpha + 1 + U_1]\psi_{k1}}{\{[\cos\alpha + \Lambda(1 + U_1)]^2 + \sin^2\alpha\}^{\frac{3}{2}}} \\
&\quad + \bar{\Omega}^2 \int_0^1 \exp[F(\xi)]\frac{\mathrm{d}\psi_k}{\mathrm{d}\xi}\left[\frac{\partial U}{\partial \xi} + \left(\frac{1}{2} - \frac{\partial U}{\partial \xi}\right)\left(\frac{\partial V}{\partial \xi}\right)^2\right]\mathrm{d}\xi = 0
\end{aligned} \tag{34}$$

and

$$\begin{aligned}
&M_p \int_0^1 \exp[F(\xi)]\phi_k[V'' + \alpha''(\xi + U)]\,\mathrm{d}\xi \\
&\quad + \beta^3 M_p \int_0^1 \frac{\exp[F(\xi)](V - (1/\Lambda)\sin\alpha)\phi_k}{\{[\cos\alpha + \Lambda(\xi + U)]^2 + [\Lambda V - \sin\alpha]^2\}^{\frac{3}{2}}}\,\mathrm{d}\xi \\
&\quad + M_p \int_0^1 \exp[F(\xi)]\phi_k[2(1 + \alpha')U' + (1/\Lambda)\sin\alpha \\
&\quad - (1 + \alpha')^2 V]\,\mathrm{d}\xi + \bar{\Omega}^2 \int_0^1 \exp[F(\xi)]\frac{\mathrm{d}\phi_k}{\mathrm{d}\xi}\frac{\partial V}{\partial \xi}\left[\frac{\partial U}{\partial \xi} + \left(\frac{\partial V}{\partial \xi}\right)^2 - \left(\frac{\partial U}{\partial \xi}\right)^2\right]\mathrm{d}\xi = 0
\end{aligned} \tag{35}$$

In Eqs. (33–35), prime denotes differentiation with respect to τ. Two useful nondimensional parameters used earlier are defined as

$$\Lambda = L_0/R_E, \qquad \beta = R_G/R_E \tag{36}$$

The characteristic frequency ratio relating the axial frequencies to the Earth's spin rate is defined by

$$\bar{\Omega} = \sqrt{EA_m/(m_{\text{tot}}L_0)}/\Omega \tag{37}$$

Also,

$$U_1 = U|_{\xi=1}, \qquad \psi_{k1} = \psi_k|_{\xi=1} \tag{38}$$

and

$$F(\xi) = \frac{R_E^2}{\bar{h}R_G(1+\varepsilon_0)}\left\{\frac{3}{2} - \frac{R_G}{[R_E+\xi(1+\varepsilon_0)L_0]} - \frac{[R_E+\xi(1+\varepsilon_0)L_0]^2}{2R_G^2}\right\} \tag{39}$$

V. Analysis of the Equations of Motion

Because the displacements of the ribbon will be very small compared with the length of the ribbon, the two motions (longitudinal and transverse) are decoupled. If the values for the bulk density and modulus of elasticity of the ribbon material are assumed to be fixed, then the ribbon frequencies will be governed by the two nondimensional parameters Λ and A_m/A_0.

A. Longitudinal Oscillations of the Ribbon

The longitudinal extension of the ribbon is now examined by neglecting its transverse displacement and libration. If this is done, Eq. (34), which governs generalized coordinates A_k, becomes

$$\begin{aligned} &M_p\int_0^1 \exp[F(\xi)]\psi_k U''\,\mathrm{d}\xi + M_c\psi_{k1}U_1'' \\ &- M_p\int_0^1 \exp[F(\xi)]\psi_k(\xi+U)\,\mathrm{d}\xi - M_c\psi_{k1}(1+U_1) \\ &- (1/\Lambda)\left\{M_p\int_0^1 \exp[F(\xi)]\psi_k\,\mathrm{d}\xi + M_c\psi_{k1}\right\} \\ &+ M_p\frac{\beta^3}{\Lambda^3}\int_0^1 \frac{\exp[F(\xi)]\psi_k}{[(1/\Lambda)+\xi+U]^2}\,\mathrm{d}\xi \\ &+ M_c\frac{\beta^3}{\Lambda^3}\frac{\psi_{k1}}{[(1/\Lambda)+1+U_1]^2} \\ &+ \bar{\Omega}^2\int_0^1 \exp[F(\xi)]\frac{\mathrm{d}\psi_k}{\mathrm{d}\xi}\frac{\partial U}{\partial\xi}\,\mathrm{d}\xi = 0 \end{aligned} \tag{40}$$

If the terms associated with the gravitational force are expanded binomially and third- and higher-order terms are ignored, the equations describing the longitudinal extension of the ribbon may be expressed as

$$\mathbf{M^A A}'' + \mathbf{K^A A} = \mathbf{0} \tag{41}$$

where the elements of matrices $\mathbf{M^A}$ and $\mathbf{K^A}$ are given by

$$M_{ik}^A = M_p\int_0^1 \exp[F(\xi)]\psi_i\psi_k\,\mathrm{d}\xi + M_c\psi_{i1}\psi_{k1} \tag{42}$$

and

$$\begin{aligned} K_{ik}^A = {}&\bar{\Omega}^2\int_0^1 \exp[F(\xi)]\left(\frac{\mathrm{d}\psi_i}{\mathrm{d}\xi}\right)\left(\frac{\mathrm{d}\psi_k}{\mathrm{d}\xi}\right)\mathrm{d}\xi - M_p\int_0^1 \exp[F(\xi)]\psi_i\psi_k\,\mathrm{d}\xi \\ &- M_c\psi_{i1}\psi_{k1} - 2\left(\frac{\beta}{\Lambda}\right)^3\left\{M_p\int_0^1 \frac{\exp[F(\xi)]\psi_i\psi_k}{[(1/\Lambda)+\xi(1+\varepsilon_0)]^3}\,\mathrm{d}\xi \right. \\ &\left. + M_c\frac{\psi_{i1}\psi_{k1}}{[(1/\Lambda)+1+\varepsilon_0]^3}\right\} \end{aligned} \tag{43}$$

where both indexes i and k vary from 1 to N.

Basis functions to approximate the longitudinal extension must now be chosen. They must all be zero at the base (when $\xi = 0$) to satisfy the boundary condition. Also, to allow the counterweight to move, the basis functions must be nonzero at the space end (when $\xi = 1$). A reasonable option is to use polynomials as basis functions; thus, let

$$\psi_i(\xi) = \xi^i \tag{44}$$

The general eigenvalue problem in Eq. (41) is solved using Matlab, using the following values: $L_0 = 100,000$ km, $A_m/A_0 = 6$, $\gamma = 1300$ kg/m^3, and $E = 1000$ GPa. The corresponding values for some of the key nondimensional parameters are $M_p = 0.992$, $M_c = 0.228$, and $\bar{\Omega} = 3.8$. The nondimensional frequencies of the longitudinal modes for $N = 5$ are 4.42, 12.44, 23.61, 36.44, and 55.44 for modes 1–5, respectively. The frequencies are nondimensionalized with respect to Ω. For values of N greater than five, some of the computed frequencies are imaginary. This result occurs because matrices $\mathbf{M^A}$ and $\mathbf{K^A}$ become very ill-conditioned as the value of N increases. As such, the results for the longitudinal frequencies and mode shapes are reliable only for $N < 6$. The first mode of longitudinal extension has a nondimensional frequency of 4.42 (i.e., a period of approximately 5.5 h). The frequencies of mode 2 through mode 5 increase in a quasi-linear fashion.

The modal matrix consisting of normalized eigenvectors along the columns, which correspond to the mode shapes of the preceding frequencies, is presented in Table 1. If the modal matrix were the identity matrix, it could be concluded that the polynomial basis functions were, in fact, the actual mode shapes of the longitudinal extension. Because the modal matrix appears very full, the basis functions are very different from the actual modes; this helps to explain, to some extent, why the mass and stiffness matrices became ill-conditioned as N was increased.

To determine a greater number of frequencies, the analysis is repeated using basis functions defined by

$$\psi_i(\xi) = \sin[(i-1/2)\pi\xi] \tag{45}$$

Clearly, the preceding basis functions satisfy the boundary condition at the base, while allowing the counterweight to move. These basis functions allow many more modes to be analyzed accurately than did the polynomials. The first 20 nondimensional natural frequencies are given in Table 2. The first five frequencies are close to those obtained in the first analysis. The quasi-linear increase in frequency continues throughout all of the examined modes. The deviations from the linear relationship may be due to the taper function of the ribbon.

Rather than presenting the 20 corresponding eigenvectors, the modal matrix obtained from a five-mode modal analysis is presented in Table 3. Because the diagonal terms are by far the largest, it may be concluded that the sinusoidal basis functions given by $\sin[(i-1/2)\pi\xi]$ correspond reasonably well to the actual mode shapes of the longitudinal motion; this is why the modal analysis could be carried out for a high number of modes. It is useful to note that the modal frequencies and mode shapes of the longitudinal motion are independent of A_m.

B. Transverse Oscillations of the Ribbon

The transverse displacement of the ribbon is now examined by neglecting its longitudinal extension (other than its nominal value given by $U = \varepsilon_0\xi$). However, the libration of the ribbon must be included in the analysis, because it represents the zeroth mode of transverse motion, or the pendulum mode. If ribbon libration is

Table 1 Modal matrix of longitudinal modes (using polynomials as basis functions)

0.11	0.11	−0.21	−0.06	0.02
−0.34	−0.37	0.66	0.36	−0.21
0.67	0.64	−0.20	−0.73	0.61
−0.61	−0.62	−0.60	0.56	−0.71
0.21	0.23	0.35	−0.13	0.29

Table 2 Nondimensional frequencies of longitudinal modes (using sinusoidal basis functions)

Mode no.	Freq.	Mode no.	Freq.	Mode no.	Freq.	Mode no.	Freq.	Mode no.	Freq.
1	4.39	5	47.82	9	96.50	13	145.27	17	194.30
2	12.48	6	59.94	10	108.62	14	157.37	18	206.43
3	23.75	7	72.14	11	120.87	15	169.72	19	219.19
4	35.69	8	84.27	12	132.98	16	181.83	20	231.55

Table 3 Modal matrix of longitudinal modes for $N = 5$ (using sinusoidal basis functions)

0.998	0.332	−0.326	0.209	−0.143
0.017	0.930	0.372	−0.232	0.168
0.062	−0.090	0.850	0.322	−0.180
0.008	0.128	−0.108	0.886	0.264
0.020	−0.014	0.144	−0.120	0.922

included and higher-order terms and damping terms are neglected, the coupled system of equations governing the libration [Eq. (33)] and generalized coordinates B_k [Eq. (35)] may be written as

$$\mathbf{M^B B}'' + \mathbf{K^B B} = \mathbf{0} \tag{46}$$

where

$$\mathbf{B} = [\alpha, B_1, B_2, \ldots, B_k]^T \tag{47}$$

and the elements of matrices $\mathbf{M^B}$ and $\mathbf{K^B}$ are given by

$$M^B_{11} = (1+\varepsilon_0)^2\left(M_p \int_0^1 \exp[F(\xi)]\xi^2\,\mathrm{d}\xi + M_c\right) \tag{48}$$

$$K^B_{11} = (1+\varepsilon_0)\left[\frac{1}{\Lambda}\left\{M_p\int_0^1 \exp[F(\xi)]\xi\,\mathrm{d}\xi + M_c\right\} - \frac{\beta^3}{\Lambda^4}\left\{M_p\int_0^1 \frac{\exp[F(\xi)]\xi}{[(1/\Lambda)+\xi(1+\varepsilon_0)]^3}\,\mathrm{d}\xi + M_c\frac{1}{[(1/\Lambda)+1+\varepsilon_0]^3}\right\}\right] \tag{49}$$

$$M^B_{i1} = M^B_{1k} = M_p(1+\varepsilon_0)\int_0^1 \exp[F(\xi)]\xi\phi_i\,\mathrm{d}\xi \tag{50}$$

$$K^B_{i1} = K^B_{1k} = M_p\left\{\frac{1}{\Lambda}\int_0^1 \exp[F(\xi)]\phi_i\,\mathrm{d}\xi - \frac{\beta^3}{\Lambda^4}\int_0^1 \frac{\exp[F(\xi)]\phi_i}{[(1/\Lambda)+\xi(1+\varepsilon_0)]^3}\,\mathrm{d}\xi\right\} \tag{51}$$

$$M^B_{ik} = M_p\int_0^1 \exp[F(\xi)]\phi_i\phi_k\,\mathrm{d}\xi \tag{52}$$

and

$$K^B_{ik} = \pi^2(\varepsilon_0 - \varepsilon_0^2)ik\bar{\Omega}^2\int_0^1 \exp[F(\xi)]\frac{\mathrm{d}\phi_i}{\mathrm{d}\xi}\frac{\mathrm{d}\phi_k}{\mathrm{d}\xi}\,\mathrm{d}\xi + M_p\left\{\left(\frac{\beta}{\Lambda}\right)^3\int_0^1 \frac{\exp[F(\xi)]\phi_i\phi_k}{[(1/\Lambda)+\xi(1+\varepsilon_0)]^3}\,\mathrm{d}\xi - \int_0^1 \exp[F(\xi)]\phi_i\phi_k\,\mathrm{d}\xi\right\} \tag{53}$$

where indexes i and k vary from 2 to $M+1$.

The basis functions are chosen as $\phi_i(\xi) = \sin(i\pi\xi)$, which vanish at the two ends of the ribbon. Again, the generalized eigenvalue problem defined by Eq. (46) may be solved using Matlab. The system parameters used for the analysis of the longitudinal oscillations are used again here. Table 4 contains the nondimensional natural frequencies for the first 20 modes of the transverse displacement of the ribbon (again, they are nondimensionalized with respect to Ω). The first frequency (zeroth mode) is that of the libration, which has a value of 0.16; this corresponds to a period of about six days. The next mode of transverse vibration has a period of about 10 h. Again, the frequencies of the transverse modes (except the rigid-body mode) increase in a quasi-linear fashion.

The modal matrix for the $M = 4$ case (four elastic modes, one rigid-body mode) is presented in Table 5. The diagonal terms of the modal matrix consisting of normalized eigenvectors are again the largest, which means that the pendulum mode and sinusoidal basis functions given by $\sin(i\pi\xi)$ are, approximately, the actual mode shapes for the transverse motion of the ribbon. It is apparent from the modal matrix that the pendulum mode has some influence over the elastic transverse modes, but the reverse may not be said. Reference [9] discusses the sinusoidal mode shapes associated with the transverse displacement of the ribbon. Their results for elastic transverse-mode shapes are $\sin(i\pi\xi)$, where $i \cong 1, 2, 3\ldots$, which agrees well with the preceding findings. However, the zeroth mode in their study was found to be $\sin(0.34\pi\xi)$, which is not a true rigid-body mode. Strangely, in their study, the period of this zeroth mode was found to be about one day. However, this study (and that of [8]) found the librational period to be around six days.

The longitudinal-to-transverse-frequency ratio of the first elastic mode is about two. This ratio increases for all subsequent modes. As

Table 5 Modal matrix of transverse modes for $M = 4$

1.000	−0.490	0.327	−0.234	0.179
0.019	0.872	−0.287	0.214	−0.115
0.009	−0.001	0.900	−0.138	0.139
0.005	0.013	−0.015	0.938	−0.085
0.004	0.007	0.023	−0.021	0.963

Table 4 Nondimensional frequencies of transverse modes

Mode no.	Freq.	Mode no.	Freq.	Mode no.	Freq.	Mode no.	Freq.	Mode no.	Freq.
0	0.16	4	8.92	8	17.74	12	26.57	16	35.41
1	2.37	5	11.13	9	19.95	13	28.78	17	37.62
2	4.53	6	13.33	10	22.15	14	30.99	18	39.84
3	6.72	7	15.53	11	24.36	15	33.19	19	42.05

was the case for the longitudinal motion, the modal frequencies and mode shapes of the transverse motion are independent of A_m.

VI. Conclusions

An analytical study was conducted to investigate the elastic longitudinal and transverse oscillations of the space elevator ribbon. For the longitudinal motion, the modal analysis was more complete when sinusoidal functions $\sin[(i-1/2)\pi\xi]$ were used as basis functions instead of the polynomials ξ^i. The period of the first mode was about 5.5 h when typical system parameters were assumed. The modal analysis for the transverse motion used the basis functions given by $\sin(i\pi\xi)$. These basis functions coupled with the rigid-body, or pendulum, mode turned out to be close to the actual mode shapes for the transverse motion. The pendulum mode of the ribbon was found to be about six days. The next lowest frequency of transverse vibration was found to have a period of about 10 h.

References

[1] Tsiolkovsky, K. E., *Speculations Between Earth and Sky*, Akademiia Nauk SSSR, Moscow, 1895, p. 35; reprint, Akademiia Nauk SSSR, Moscow, 1959.

[2] Artsutanov, Y., "To Space by a Locomotive," *Komsomolskaya Pravda*, 31 July 1960.

[3] Isaacs, J. D., Vine, A. C., Bradner, H., and Bachus, G. E., "Satellite Elongation into a True Skyhook," *Science*, Vol. 151, Feb. 1966, pp. 682–683.

[4] Pearson, J., "The Orbital Tower: A Spacecraft Launcher Using the Earth's Rotational Energy," *Acta Astronautica*, Vol. 2, Nos. 9–10, 1975, pp. 785–799.

[5] Iijima, S., "Helical Microtubules of Graphitic Carbon," *Nature*, Vol. 354, No. 6348, 1991, pp. 56–58.

[6] Edwards, B. C., "Design and Deployment of a Space Elevator," *Acta Astronautica*, Vol. 47, No. 10, 2000, pp. 735–744.

[7] McInnes, C. R., "Dynamics of a Particle Moving Along an Orbital Tower," *Journal of Guidance, Control, and Dynamics*, Vol. 28, No. 2, 2005, pp. 380–382.

[8] Lang, D. D., "Space Elevator Dynamic Response to In-Transit Climbers," 1st International Conference on Science, Engineering, and Habitation in Space, Albuquerque, NM, Space Engineering and Science Inst., Paper 10152148, 2006.

[9] Patamia, S. E., and Jorgensen, A. M., "Analytical Model of Large Scale Transverse Dynamics of Proposed Space Elevator," 56th International Astronautical Congress of the International Astronautics Federation, Fukuoka, Japan, International Astronautical Congress Paper 05-D4.2.06, 2005.

[10] Yakobson, B. I., and Smalley, R. E., "Fullerene Nanotubes: C1000,000 and Beyond," *American Scientist*, Vol. 85, No. 4, 1997, pp. 324–337.

[11] Min, B. N., Misra, A. K., and Modi, V. J., "Nonlinear Free Vibration of a Spinning Tether," *The Journal of the Astronautical Sciences*, Vol. 47, Nos. 1–2, 1999, pp. 1–23.